

Waveguide grating for microchip-laser polarization control

Florent Pigeon (1), Marwan Abdou Ahmed (2), Olivier Parriaux (1), Svetlen Tonchev (3),
Nicolas Landru (4) and Jean-Philippe Fève (5)

(1) Laboratoire Hubert Curien (formerly TSI) UMR CNRS 5516, 18 Rue B. Laurus, F-42000 Saint-Etienne

(2) Institut für Strahwerkzeuge (IFSW), Stuttgart University, Pfaffenwaldring 43, D-70569 Stuttgart

(3) on leave from the ISSP, Sofia, Bulgaria

(4) Teem Photonics, 61 Ch. du Vieux Chêne, 38246 Meylan, France

(5) JDSU Laser Products Group, 430 North McCarthy Blvd., Milpitas CA 95035, USA

parriaux@univ-st-etienne.fr

Abstract: *A slab waveguide grating submirror monolithically associated with a standard multilayer submirror represents a laser output coupler which polarizes the emission of a passively Q-switched Nd:YAG microchip laser over its full emission bandwidth by intra-mirror destructive interference for the undesired polarization. A polarization extinction ratio of more than 25 dB is obtained up to 6.1 μJ pulse energy. Linearly polarized emission shows no loss penalty.*

Introduction

In most applications of surface emitting lasers such as disk and microchip lasers or VCSELs, there is a need for an integrated element which controls the emitted polarization. The planar geometry of such lasers forbids the use of a Brewster element. Since the discovery [1] and analysis [2] of the effect of zeroth order resonant reflection from a grating slab waveguide, it is possible to achieve the polarization control of laser emission by highly polarization selective reflection as first demonstrated by Sychugov et al [3] in the case of a semiconductor laser with external cavity mirror. Zeroth-order resonant reflection can theoretically reach 100% for one polarization [4].

The present paper demonstrates a laser polarizing mirror solution which takes the best of two mirror technologies: the well established non-selective multilayer technology which ensures most of the needed reflection, and the corrugated slab technology which does not reflect much light but essentially produces the polarization selectivity. Stimulated emission does the rest by amplifying the sole polarization which experiences the larger reflection coefficient. The specific feature in the present combination of the multilayer and resonant submirrors is the destructive interference condition between fields which each submirror reflects which implies that it is the polarization which experiences resonant reflection which is filtered out.

This is not the only approach for monolithically polarizing laser emission by means of a periodic structure: the combination between each submirror can have a constructive character and lead to the lasing of the polarization experiencing waveguide coupling and resonant reflection [5]; there are important differences in terms of bandwidth and power flux resistance. There are other polarizing mechanisms as well: a deep binary grating etched into a thick high index layer can exhibit 100% reflectivity for the TM polarization according to the GIRO mirror scheme [6]. A shallow grating of relatively large period can also induce a reflection differential as demonstrated in VCSELs [7]; such an approach is however risky as a large period gives rise to propagating diffraction orders or couples the emitted wave to unforeseeable guided modes of the multilayer whose density may be large. Another, more predictive approach, uses deep trenches into the multilayer with the objective of giving rise to photonic crystal effects [8]; the risk here is the scattering losses associated with an imperfect trench pattern of very high index contrast. The present approach excites a well identified mode of the multilayer without losing power in radiated diffraction orders and it is much less traumatic than a photonic crystal to the mirror and photon generation process, since it is a soft post-process on top of an essentially standard multilayer.

Associating multilayer and resonant submirrors

The multilayer submirror ensures a low-loss, high-reflection pedestal, whereas the resonant mirror adds its polarization selectivity to the smaller part of the reflection it provides. The reflection pedestal provided by the multilayer submirror is set at the reflection level needed for laser operation of the desired polarization whereas the reflection dip due to waveguide coupling and resonant reflection must have a depth below threshold to prevent the amplification of the undesired polarization. The

sketch of the superposition of the two submirrors is shown in Fig. 1.

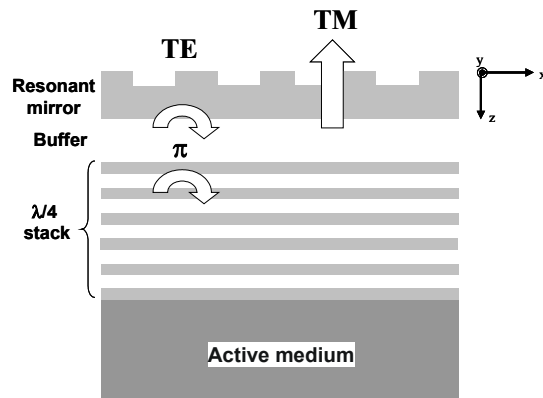


Fig. 1: Destructive interference polarizing mechanism resulting from the association of a multilayer submirror and a polarization selective resonant submirror.

The two submirrors are separated by a low-index buffer, whose thickness w_b is adjusted on the basis of the following criteria: first, the buffer layer thickness dictates the phase shift $\Delta\phi$ between the field reflected by the multilayer and that reflected by the resonant grating. If the grating is made at the cover side of the mirror (usually at the air side), $\Delta\phi$ is given by

$$\Delta\phi = 2k_0(n_b w_b + n_w w_w) + \pi \quad (1)$$

where $k_0 = 2\pi/\lambda$ is the wave number in the cover (here considered as air), n_b and n_w are the refractive index of the buffer and waveguide slab layers of thickness w_b and w_w respectively. The last term of expression (1) is the phaseshift upon resonant reflection known to be π [4]. In the present case $\Delta\phi$ must be close to π modulo 2π for destructive interference between the multilayer and resonant submirror reflected fields as illustrated in Fig. 1: the polarization which is coupled to the slab waveguide does not lase since its reflection coefficient is decreased by destructive interference.

Design of the polarization selective mirror

As a practical example for the implementation of such a device, the polarizing function will be monolithically integrated into the multilayer mirror of a passively Q-switched microchip laser (Nd:YAG as the gain medium, bonded to a Cr:YAG saturable absorber).

The incidence is from the substrate side as suggested in Fig. 1. The substrate index at the emission wavelength of 1064 nm is $n_s = 1.82$. The multilayer mirror technology is $\text{HfO}_2/\text{SiO}_2$ ion plating with

assumed layer refractive indices of 2.10/1.48. The targeted reflection coefficient of the laser output coupler for the lasing polarization, i.e. the multilayer pedestal, is set at about 85%, whereas the polarization selective resonant dip is set at 60% reflection at most to prevent the lasing of the undesired polarization.

An approximate design essentially defined by expression (1) is fed into a grating optimization code based on the modal method which searches for the desired dichroic properties of the polarization filter.

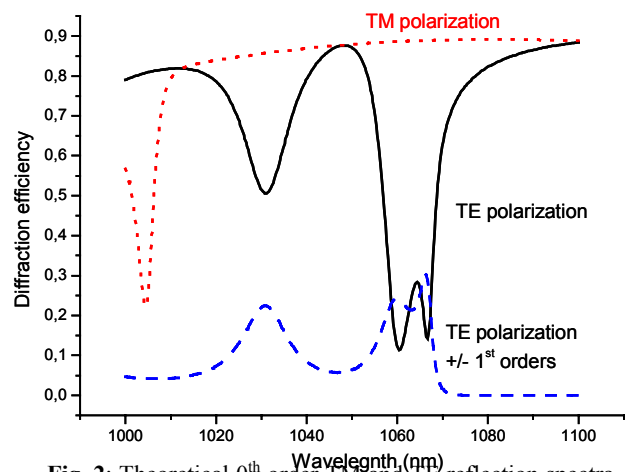


Fig. 2: Theoretical 0th order TM and TE reflection spectra and reflected $\pm 1^{\text{st}}$ order TE diffraction efficiency with excitation from the substrate side.

Figure 2 gives the TE and TM reflection spectra of the optimized resonant grating multilayer. The grating is a binary corrugation of 605 nm period, 145 nm depth and 1/1 line/space ratio. The optimised thickness of the low index SiO_2 buffer is 400 nm. Figure 2 gives the theoretically expected TM and TE reflection spectra as well as the $\pm 1^{\text{st}}$ order TE reflection into the active substrate with incidence from the active substrate side. As expected, it has been possible to bring two neighbouring TE modes close to 1064 nm which permits to considerably broaden the tolerances. Their effective index is $n_e = \lambda/\Lambda = 1.776$ and 1.767. Plotting the electric field of these two modes reveals that the dominant modal field ($n_e = 1.776$) has no zero crossing and is the fundamental mode of the whole structure. The closely neighbouring mode with $n_e = 1.767$ with its single zero crossing is the TE_1 mode.

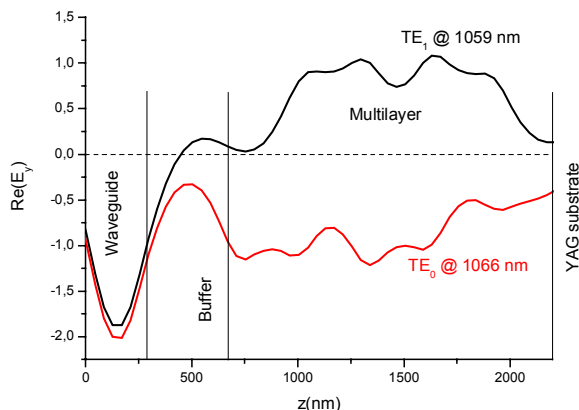


Fig. 3: Calculated electric field distribution of the two neighboring lowest order TE modes of the optimized structure giving rise to the spectra of Fig. 2.

Figure 3 illustrates the electric field profile of these two modes at their resonance wavelength. As intended from the start, both fields exhibit a strong maximum in the high index waveguiding layer and a slow decrease at the substrate side. One understands now why it was possible to bring the effective index of these two modes close to each other: thanks to the wide low index buffer layer the structure is equivalent for the two first order modes to a directional coupler with its two supermodes of neighbouring effective index, the first waveguide being the last high index waveguiding layer, the second waveguide being the rest of the multilayer.

Fabrication of the grating multilayer.

The prescribed $\text{SiO}_2/\text{HfO}_2$ multilayer was deposited onto 12.5 mm diameter, 1.23 mm thick Nd:YAG wafers bonded to a 0.33 mm thick Cr:YAG saturable absorber. The resist-coated wafers were exposed according to the design to a 605 nm period interferogram at 442 nm wavelength. The physical transfer was made by a RIBE process using a 60% CF_4 and 40% argon ion beam.

The corrugated multilayer was submitted to the incidence of a polarized microchip Nd:YAG laser beam at 1064 nm wavelength in the neighbourhood of normal incidence with incidence from the air side. Figure 4 gives the reflected power measured for both polarizations upon a variation of the incidence angle. As expected the reflected TM polarization exhibits a monotonic angular dependence since there is no TM resonance in this region. The TE polarization shows a pronounced reflection fall in the form of one wide dip at either side of the normal. As a whole there is a polarization eye between the TE and TM polarizations exhibiting a TE reflection coefficient at

least 20% smaller than the TM's over a full angular range $\Delta\theta$ of about 3.4 degrees. Under close to normal incidence, and neglecting the wavelength dependence of the effective index, this corresponds to a wavelength range $\Delta\lambda = \Lambda\Delta\theta = 18$ nm which covers well over the Nd:YAG gain bandwidth which is about 0.6 nm.

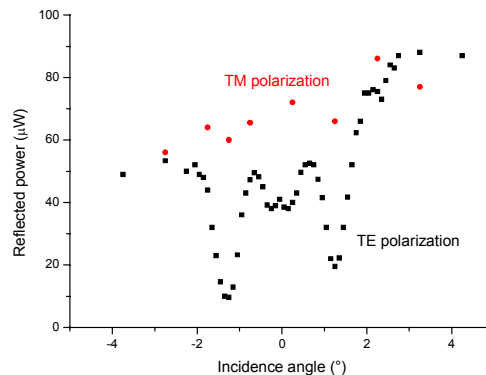


Fig. 4: TE and TM reflected power at 1064 nm versus incidence angle measured upon incidence from the air side.

The wafer scale uniformity was tested by AFM scans made at 5 different places: the grating depth is 143 nm within 5 nm, and the line/space ratio is 1.0 ± 0.1 . Systematic but low sensitivity scattering measurements have been performed on such a device by directing the collimated beam of a filtered white light source onto the grating region from the substrate side. The scattering level is evaluated on the reflected beam by repeatedly moving the grating area into and outside the beam cross section. The results reveal that the scattering level on the reflected TE polarization (that which couples the guided mode) is at most 0.6%, the scattering measurement being made outside the reflection dip at 1056 nm wavelength, and that the scattering of the reflected TM polarization (the lasing polarization) is at most 0.14%, the scattering measurement being made at the wavelength of the TE reflection dip.

Laser experiments

Pumping was achieved with a multimode diode at 808 nm ($1 \times 100 \mu\text{m}$ emitter, linear horizontal polarization). The pump power incident on the laser cavity was 0.8 W, focused by a gradient-index lens into a beam size of $60 \mu\text{m}$. Before etching the grating, the repetition rate was 10.4 kHz, the pulse energy 5.9 μJ , and the pulse duration 0.59 ns. After processing the grating, the frequency was 11.16 kHz and the

pulse energy 6.1 μ J. This shows that the process did not degrade the multilayer coating. This is also highly consistent with the above scattering measurements: in the considered Nd:YAG microlasers, the loss penalty due to the grating itself is at least two orders of magnitude lower compared with the other passive losses of the laser cavity (output coupling and non-saturable absorption of the passive Q-switch). As a consequence, this additional loss does not play any noticeable role on the laser performance.

We measured the polarization of the 1064 nm output beam before etching the grating. The output polarization was partially linear, and we rotated the wafer to maximize the polarization extinction ratio (PER), which corresponds to the preferred orientation always horizontal, similar to the pump. We marked this preferred axis on the wafer as a guide for the alignment of the grating. Without grating, the PER was very inhomogeneous throughout the surface of the wafer, ranging from 4 dB to 34 dB; at the center of the wafer, measurements on four wafers varied from 11 dB to 33 dB. These huge variations confirm that an external mean is needed to obtain reproducible controlled output polarized beam from a microlaser.

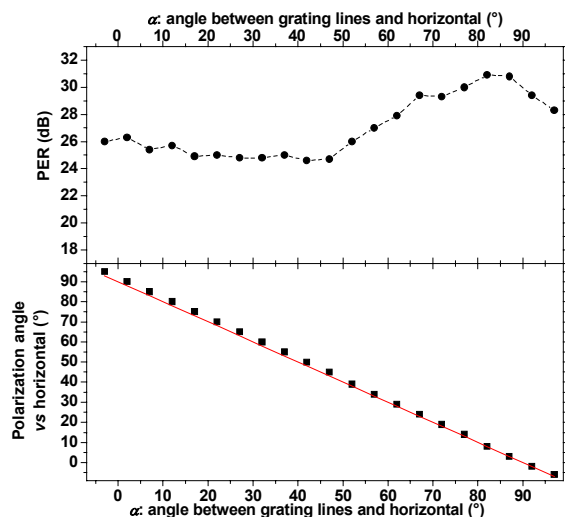


Fig. 5: Bottom curve: direction of polarization (measured from horizontal) vs angle α between the grating lines and the horizontal. The top curve represents the corresponding variation of the PER.

Figure 5 shows the polarization data measured at the center of the wafer after etching the grating. First, the PER is larger than 25 dB whatever the angle α between the grating and the horizontal axis (i.e.

orientation of grating lines with respect to the polarization of the pump diode). Second, the polarization of the output beam is at 90° from the lines of the grating for every orientation of the wafer. These data clearly demonstrate that the grating ensures an efficient control of the polarization of the laser beam.

Conclusion

This paper reports on the demonstration of the monolithic control of the polarization emitted by a microchip laser by means of a waveguide grating effect suppressing the emission of the undesired polarization. An appropriate division of functions between a standard multilayer submirror and a post-processed two-layer waveguide submirror combines the low-loss feature of laser mirror technology and the polarization selectivity of resonant reflection, the latter causing the destructive interference of the two submirror reflected fields. The power flux resistance of the microchip laser is hardly affected by the action of the resonant grating since the latter only acts on the non-lasing polarization. For the same reason, grating scattering affects the lasing polarization only marginally.

Acknowledgement

The authors thank J.Cl. Pommier and S. Reynaud for performing the RIB-etching and the AFM scans. The support of the RMNT under the Micropack project is gratefully acknowledged.

References

- 1 V. N. Bel'tyugov et al., Proc. SPIE, vol. 1782, p. 206, 1992.
- 2 L. Mashev et al., Opt. Commun., vol. 55, p. 377, 1985.
- 3 G. A. Golubenko et al, Sov. J. Quantum Electron., vol. 15, p. 886, 1985.
- 4 I. A. Avrutsky et al., J. Mod. Opt., vol. 36, p. 1527, 1989.
- 5 J.-F. Bisson et al., Appl. Phys. B: Lasers and Optics, vol. 85, p. 519, 2006.
6. S. Goeman et al., IEEE Photon. Technol. Lett., vol. 10, p. 1205, 1998.
7. J. M. Ostermann, et al., IEEE Photon. Technol. Lett., vol. 17, 2505, 2005.
8. Dae-Sung Song et al., Appl. Phys. Lett., vol. 82, p. 3182, 2003.